Detecting lightning infrasound using a high-altitude balloon

Oliver D. Lamb[1], Jonathan M. Lees[1], Daniel C. Bowman[2]

[1]Department of Geological Sciences, The University of North Carolina at Chapel Hill, Chapel Hill, North Carolina, USA
[2]Sandia National Laboratories, Albuquerque, New Mexico, USA

Key Points:

- First lightning infrasound detected using free-flying balloon at stratospheric altitudes over Tasman Sea in May 2016.
- Infrasonic signals matched with a few lightning strokes within 100 km range of balloon as it flew over at least two thunderclouds.
- Strong atmospheric effects likely reduced the number of recorded signals generated by lightning strokes within range of the balloon.

Corresponding author: Oliver Lamb, `olamb@email.unc.edu`

Abstract

Acoustic waves with a wide range of frequencies are generated by lightning strokes during thunderstorms, including infrasonic waves (0.1 to 20 Hz). The source mechanism for these low frequency acoustic waves is still debated and studies have so far been limited to ground-based instruments. Here we report the first confirmed detection of lightning generated infrasound with acoustic instruments suspended at stratospheric altitudes using a free-flying balloon. We observe high-amplitude signals generated by lightning strokes located within 100 km of the balloon as it flew over the Tasman Sea on 17 May 2016. The signals share many characteristics with waveforms recorded previously by ground-based instruments near thunderstorms. The ability to measure lightning activity with high-altitude infrasound instruments has demonstrated the potential for using these platforms to image the full acoustic wavefield in the atmosphere.

Plain-language summary

Lightning generates sound waves across a wide range of frequencies, including below the threshold for human hearing at 20 Hz. How these waves at less than 20 Hz, also known as infrasound waves, are generated during a lightning stroke is currently an area for debate. So far, measurements of lightning infrasound waves have been limited to microphones fixed to the ground and models have shown that only a small section of sound waves actually reach the ground. Here we show lightning infrasound that has been detected using microphones suspended over a thunderstorm using a balloon flying at 32 km height. This opens up the possibility of using balloons in future studies to make better measurements of infrasound waves generated by lightning activity and in turn, give a better idea of how they are generated.

1 Introduction

Acoustic signals with frequencies between 0.02 to 20 Hz are classified as infrasound and are not audible to humans. A wide variety of sources have been found to generate infrasound, including: volcanoes, earthquakes, avalanches, tsunami, meteors, aurora, thunderstorms, wind-mountain interactions, supersonic aircraft, rockets, and chemical and nuclear explosions [*Campus and Christie*, 2010]. Infrasonic signals can travel hundreds to thousands of kilometers through the atmosphere, sampling areas from the Earth's surface up to the thermosphere. A variety of institutions maintain arrays for monitoring purposes, such as volcano observatories [*Fee and Matoza*, 2013] or the International Monitoring System [*Christie and Campus*, 2010]. The vast majority of infrasound studies currently use ground-based instrument arrays and networks. Infrasound instruments deployed on the ground may be subject to high-levels of background noise which may obscure the signals of interest, or the signals may arrive distorted due to topographic or atmospheric propagation effects [e.g. *Lacanna and Ripepe*, 2013; *Kim and Lees*, 2014]. Furthermore, the intensity of the acoustic wavefield may be as much as 50% greater directly above the source compared that at a similar horizontal distance [*Blackstock*, 2000].

A series of studies have recently taken place to explore how to fill this gap in our ability to monitor the atmospheric acoustic wavefield. These experiments have tested the use of microphones suspended underneath free-floating balloons to record infrasound at high-altitude [e.g. *Bowman and Lees*, 2015, 2017; *Bowman and Albert*, 2018]. Balloon deployments conducted as part of the NASA High-Altitude Student Platform (HASP) program described evidence of the ocean microbarom as well as other signals of unknown provenance [*Bowman and Lees*, 2015]. A follow-up experiment showed that the ocean microbarom was often detectable in the stratosphere but not at ground-level, either due to low noise at the balloons, an elevated acoustic duct, or both [*Bowman and Lees*, 2017]. In 2017, four microphone-bearing solar balloons were launched concurrently and successfully detected and located a chemical explosion on the ground [*Bowman and Albert*, 2018].

So far, none of these experiments have confirmed the detection of other infrasonic signals from sources such as lightning storms.

Acoustic emissions from lightning, described as thunder, can produce a broadband range of frequencies. The origin of the audible portion of the thunder (20-20,000 Hz) is widely understood to come mostly from shock waves produced by the rapid heating and expansion of a lightning channel due to current flow [*Few et al.*, 1967]. In addition, numerous studies have observed infrasound generated by cloud-to-ground (CG) and intracloud (IC) lightning flashes [e.g. *Balachandran*, 1983; *Assink et al.*, 2008; *Farges and Blanc*, 2010; *Arechiga et al.*, 2014]. The lightning signal is often a discrete pulse characterized by an initial compression followed by a rarefaction with maximum amplitudes in the range of 0.05 to 5 Pa and a spectral peak in the range of 0.2 to 2 Hz [*Dessler*, 1973; *Bohannon et al.*, 1977; *Assink et al.*, 2008; *Campus and Christie*, 2010]. Multiple production mechanisms have been postulated for the infrasonic acoustics detected during lightning storms. This includes rapid intensification of the electric field just prior to the flash, ohmic heating of the air by charge flowing into the channel, and interaction between the positive and negative charge layers in the storm cloud [*Dessler*, 1973; *Bohannon et al.*, 1977; *Pasko*, 2009]. Furthermore, the acoustic wavefield generated by this mechanism was predicted to be orientated vertically, restricting the horizontal detection range of lightning infrasound [*Dessler*, 1973; *Pasko*, 2009]. Validation of the production mechanism and acoustic wavefield has been confounded by the difficulty in locating the charge layers in the storm cloud, as well as characterizing the structure of the parent lightning flash. Advancements in location algorithms and instruments deployments such as the Lightning Mapping Array (LMA) have produced observations that refute the previously proposed production mechanisms [*Arechiga et al.*, 2014]. Instead, the observations suggest that the infrasonic signals from lightning flashes may be produced by electrostatic interaction of charge deposited in the streamer zone of a lightning channel [*Arechiga et al.*, 2014]. Lightning infrasound has also been detected at ranges of up to 150 km from the source, contrary to previous predictions of a vertically orientated acoustic wavefield [e.g. *Farges and Blanc*, 2010].

Here we report on detections of lightning infrasound recorded by a high-altitude balloon flying over the Tasman Sea on 17 May 2016. We present evidence for signals recorded from at least two groups of lightning flashes during a 6 hour period. Measurements suggest that the detection of lightning infrasound was limited by the distance and atmospheric conditions between source and receiver. A few example signals from lightning strokes are isolated and their waveform characteristics are briefly discussed. These observations, the first of their kind reported, suggest that microphones deployed on high-altitude balloons can offer additional insights into the production mechanisms of lightning infrasound.

2 Data

An acoustic sensor package was included as a piggyback payload on the NASA Ultra Long Duration Balloon (ULDB) flight launched from Wanaka, New Zealand on 16 May 2016. The ULDB landed in Peru on 2 July 2016 for a total flight duration of 46 days. The ULDB balloon position and height was recorded using an onboard GPS unit, and records show the full flight included a full circumnavigation of the southern hemisphere [*Bowman et al.*, 2017]. The acoustic sensor package recorded data for the first 20 days of the flight, and the ocean microbarom was recorded throughout as well as other signals of unknown provenance [*Bowman and Lees*, 2018].

The sensor package contained three InfraBSU microphones [*Marcillo et al.*, 2012]: one control and a pair with reversed polarities. The reversed polarity sensor was achieved by placing the mechanical sensor on the opposite port. The reversed polarity microphone pair were combined into a single channel via:

$$M = \frac{M_+ - M_-}{2} \tag{1}$$

where M is the data analyzed in this article, and M_+ and M_- are the data from the microphones with positive and negative polarities, respectively. The control sensor was a microphone that was disabled by removing the mechanical filter entirely. This acoustic sensor trio was designed to robustly distinguish between true pressure fluctuations and spurious signals, such as electronic interference [*Bowman et al.*, 2017]. Data was recorded at 200 samples per second at 64x gain using an Omnirecs Datacube digitizer. The microphones were not calibrated to the pressure and temperature conditions experienced during the flight, but their primary effect should be to lower the corner period of the sensors [*Bowman et al.*, 2017]. The acoustic waveforms presented here are high-pass filtered at 0.6 Hz in order to remove high-amplitude signals contributed from the ocean microbarom [*Bowman and Lees*, 2018], atmospheric gravity waves generated by thunder cloud convection [*Blanc et al.*, 2010], and balloon oscillations [*Anderson and Taback*, 1991]. (Unfiltered signals recorded by the acoustic package can be seen in Figure S1 in supplementary information.) The microphones and digitizer were each powered by separate Lithium battery packs, and contained within high density styrofoam shipping boxes for thermal insulation. Internal temperatures within the digitizer ranged from -26 to 7 °C during the flight.

The lightning stroke detections and location data used in this article were detected and recorded by the World Wide Lightning Location Network (WWLLN). The WWLLN is an instrument network capable of locating and timing lightning strokes at long range (thousands of kilometers) to within <10 km and <10 μs [*Hutchins et al.*, 2012]. The network uses very-low-frequency radio wave (3-30 kHz) receivers distributed around the globe to identify the time of group arrival for individual lightning waveforms, or sferics. The network is capable of detecting both CG and IC discharges, but the latter are typically underrepresented in detection databases as they produce weaker electromagnetic pulses [*Behnke and McNutt*, 2014]. As of 2010, the estimated detection efficiency for the network was ∼11% for all strokes and >30% for more powerful strokes [*Hutchins et al.*, 2012]. These values may seem low, but the WWLLN was not designed to detect all lightning strokes but instead to provide a global overview of lightning activity [*Dowden et al.*, 2008].

3 Observations

The ULDB was launched from Wanaka, New Zealand just before 0000 UTC on 17 May 2016 started flying east as it ascended. Once the craft approached and breached 30 km altitude, it turned to the west and flew out over the Tasman Sea and towards Australia (Fig. 1). During this period, the WWLLN detected intense lightning activity from multiple thunderstorms approaching New Zealand from the west (Fig. 1, Movie S1 in supporting information). From 0800 to 1400 UTC, 2994 strokes were detected and located by the WWLLN across the Tasman Sea, of which 2554 were located within 500 km of the ULDB (Fig. 2a). At approximately 0945 and 1200 UTC the ULDB passed directly over or near lightning activity which correlates with an increase in acoustic activity recorded at the ULDB (Fig. 2a, b). Acoustic signals are recorded with peak-to-peak amplitudes of up to 0.05 Pa and a broadband range of frequencies from 0.6 to 20 Hz (Fig. 2b, c).

As the acoustic sensor package on the ULDB was fundamentally a single element station, back-azimuths and slowness vectors cannot be calculated to locate sources of detected signals. To estimate detection ranges, ray tracing was used to model infrasonic propagation paths between lightning and the ULDB. Ray tracing was performed using classical geometric acoustics techniques and a plane wave assumption, calculated within the open source GeoAc ray tracing software [*Blom and Waxler*, 2012]. Rays were launched

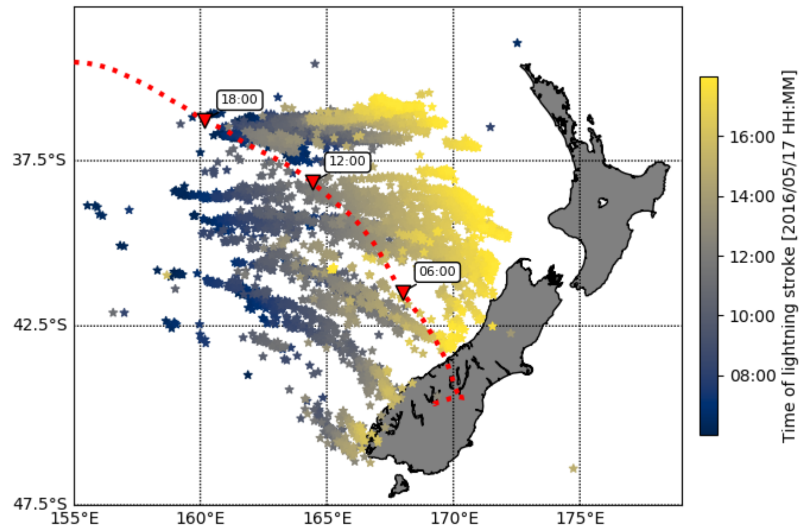

Figure 1. Map of the Tasman Sea with the locations of lightning detected by the WWLLN from 0600 to 1800 UTC on 17 May 2016, where color represents the progression of time (see colorbar). Also plotted is the path of the ULDB balloon after it was launched from Wanaka, New Zealand (red dotted line), and it's location at 0600, 1200 and 1800 UTC on 17 May 2016 (red triangles). (For an animated version of this figure, see Movie S1 in supporting information.)

at intervals of 1° from a point source at a height of 4 km. This source height was based on previously used heights for modeling lightning infrasound [*Pasko*, 2009; *Farges and Blanc*, 2010]. Atmospheric profiles was derived from the 12z Global Forecast System (GFS) analysis model run, located at the latitude/longitude coordinates for the ULDB at 1200 UTC on 17 May 2016 (Fig. S2 in supplementary information). For a source at 4 km height and a receiver at 32 km height, direct arrivals from the source should only be expected <110 km horizontal distance in all directions (Fig. 3). At this distance, 34 lightning strokes were recorded when the ULDB flew near a storm at approximately 1200 UTC (Fig. 4a). 10 strokes were recorded within 100 km during the earlier storm at 0945 UTC (Fig. S3 in supplementary information).

To match infrasonic signal peaks and specific lightning strokes, we compute the time needed for waveforms from each stroke within a limited distance to arrive at the ULDB. We take a simplified approach and assume that the atmosphere can be approximated with a bulk acoustic wave speed of 300 ms^{-1}. Furthermore, all acoustic waveforms arriving at the ULDB platform are assumed to be direct arrivals from the source. For the 34 lightning strokes within 100 km of the balloon between 1130 and 1230 UTC, only a few events appear to match directly with peaks in recorded acoustic amplitudes (Fig. 4b). Three matches occur for signals recorded at the ULDB at 1145, 1148, and 1152 UTC and are plotted in Fig. 4c, d, and e, with their respective spectrograms (Fig. 4f, g, h). None of the detected strokes directly match with infrasonic signals during the earlier storm at 0945 UTC (Fig. S3 in supplementary information). The apparent low matching rate between lightning strokes and acoustic signals indicates that recording infrasonic thunder signals at stratospheric altitudes was dependent on source-receiver distance, lightning stroke energy, and the atmospheric conditions.

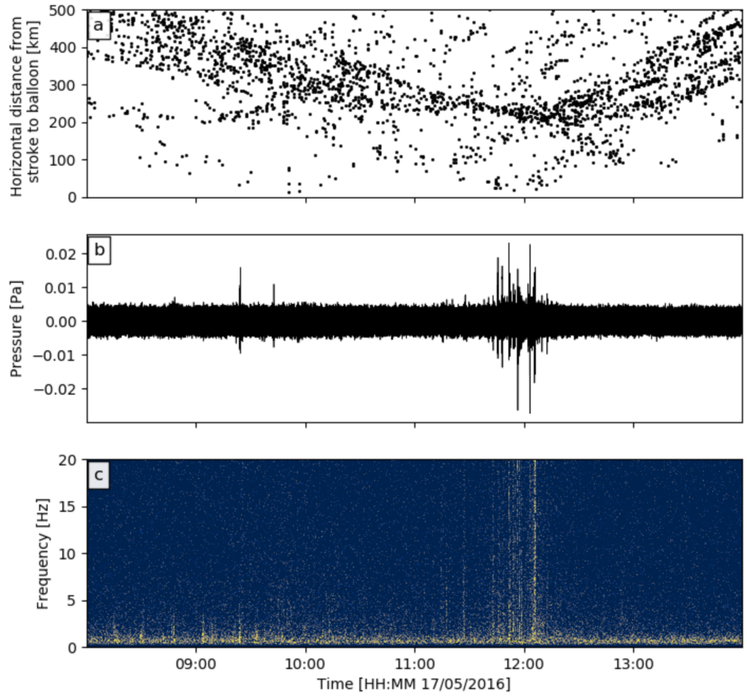

Figure 2. (a) Horizontal distances for each stroke within 500 km of the balloon's location at the time of the stroke, from 0800 to 1400 UTC on 17 May 2016. (b) High-pass filtered (0.6 Hz) infrasound over the same time period as recorded at the ULDB. (c) Frequency spectrogram of the waveform plotted in (b).

4 Discussion and Conclusions

Here we have presented evidence that lightning infrasound was observable by acoustic instruments suspended at stratospheric altitudes by free-flying balloons. Several waveforms were matched with detected lightning strokes through a simple time delay approach (Fig. 4c, d, e). Here, we have assumed that the signals represent direct arrivals between the source and receiver. To test this assumption, we searched for eigenray solutions using the GeoAc software package. Direct arrivals for all three waveforms are found for the distances and azimuths to their associated lightning strokes (Fig. S4 in supplementary info). However, the arrival times using the eigenray paths described earlier to calculate their arrival times does not readily match with the recorded arrival times of signals (Fig. S4 in supplementary information). It is worth noting that there were a number of signals recorded that do not readily match with any lightning strokes detected by the WWLLN, and *vice versa* (Fig. 4a, b). If the estimated detection rates of the WWLLN are correct [11-30%; *Hutchins et al.*, 2012], then there may have been as many as 100-300 lightning strokes within 100 km of the ULDB. This number of high-amplitude signals was not recorded at the ULDB (Fig. 4b), therefore the total number signals recorded at the ULDB underrepresents the true total of lightning strokes that occurred within range of the balloon. This is similar to detection rates of lightning infrasound by ground-based instruments [e.g. *Farges and Blanc*, 2010]. This may be attributed to very low signal-to-noise ratios, especially for smaller lightning strokes or those located further from the instru-

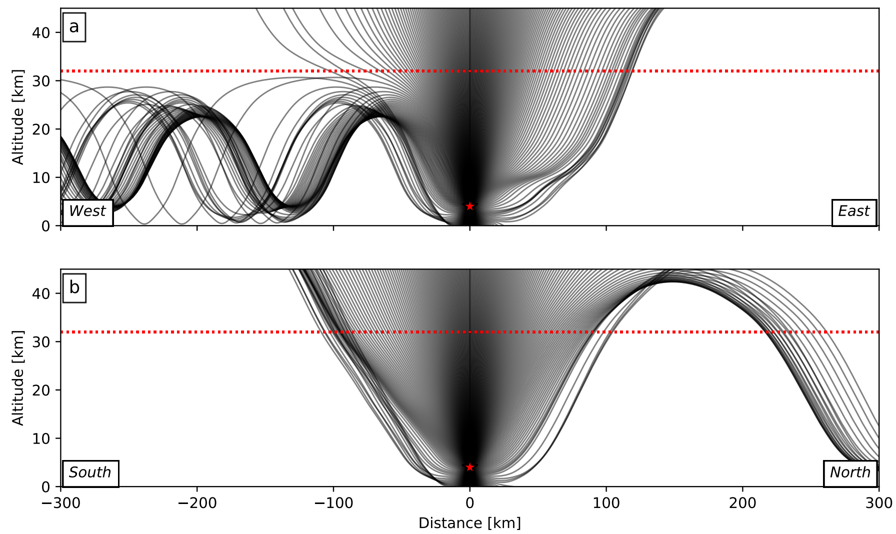

Figure 3. Ray-tracing propagation for an acoustic source (red star) at 4 km height along East-West (a) and North-South (b) profiles using realistic atmospheric conditions derived from the Global Forecast System. The red dotted line at 32 km indicates the approximate height of the ULDB balloon on 17 May 2016.

ment than the rest of the thunderstorm cloud [*Farges and Blanc*, 2010]. Complex atmospheric conditions likely refract the generated acoustic waves away from the receiver [*Jones and Bedard*, 2015]. Additionally, it is possible that not all lightning strokes generate measurable infrasound.

For the ray propagation and eigenray modeling we have assumed a point source for the lightning infrasound at 4 km altitude. Infrasound sources from lightning have been mapped as high as 12 km altitude in the thundercloud [*Anderson et al.*, 2014; *Arechiga et al.*, 2014]. Furthermore, the mapped current flow within lightning strokes suggests the source geometry can resemble complex, dendritic structures [*Anderson et al.*, 2014]. To test whether our source shape and height assumption was viable, we have repeated the ray tracing modeling but with a source at 32 km height instead, the height of the ULDB. In reverse, this can be seen as all possible locations for sources whose acoustic waveforms will be recorded at the receiver. Results suggest that a receiver at 32 km should record signals from heights up to 12 km and take-off angles between 45-90° within a 100 km horizontal range in all directions (Fig. S5 in supplementary information). Therefore, the source configuration used for the raypath modeling was reasonable for the lightning infrasound described here.

A key assumption here was that the atmospheric conditions during the generation of the lightning infrasound was relatively simple and stratified. Thunderstorms require unstable air to form and persist, and often include significant vertical wind shear due to thermal plumes. The wind and temperature profiles used for ray path modeling here was likely a highly simplified representation of reality. Ray tracing from sources directly below thermal plumes such as those found within thunderstorm clouds have shown how they may act as vertical waveguides and thus can greatly distort the acoustic wavefield [*Jones and Bedard*, 2015]. Ray paths are found to either converge or diverge at the top of the thermal plume dependent on the height and width of the plume [*Jones and Be-*

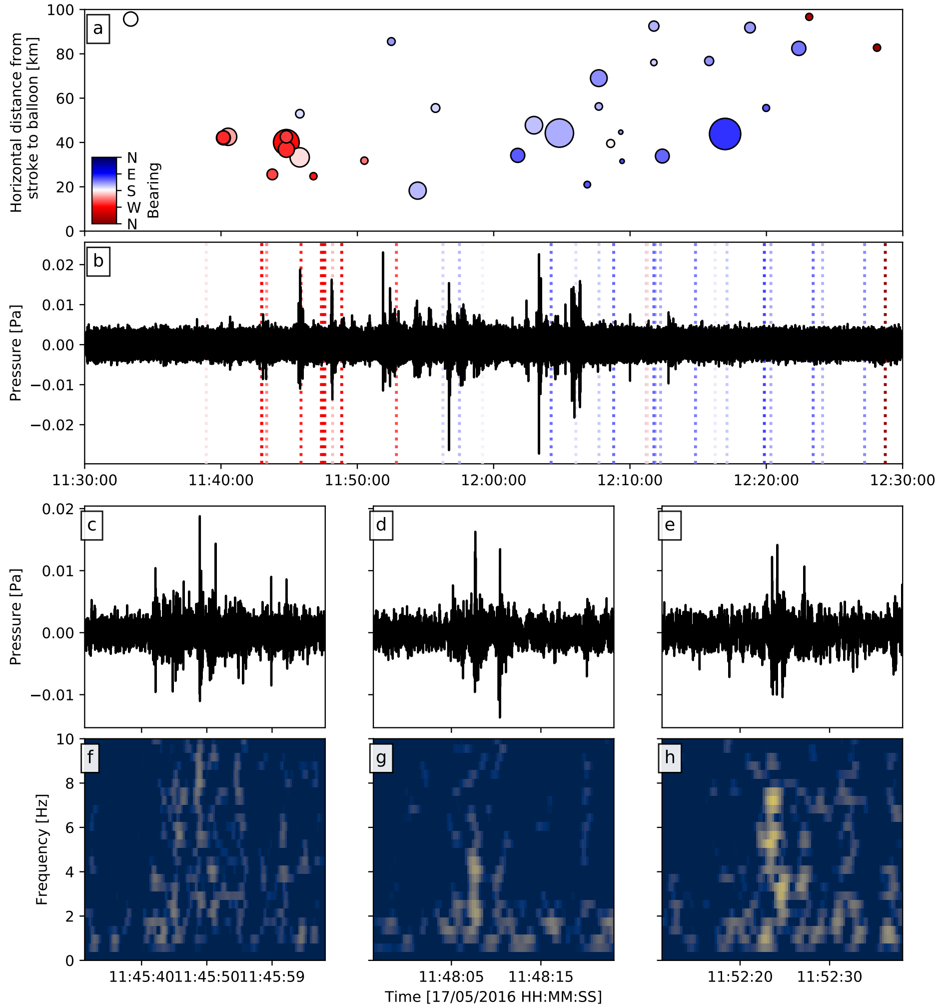

Figure 4. (a) Horizontal distances for each stroke within 100 km of the balloon from 1130 to 1230 UTC on 17 May 2016. each stroke is sized by the stroke energy, and colored by the bearing from the balloon to the stroke location. (b) High-pass (0.6 Hz) filtered acoustic waveform as recorded at the ULDB over the same time period. Vertical dotted lines indicate calculated time of arrivals for strokes in panel (a), colored by the bearing. (c,d,e) Example acoustic signals from lightning strokes and their respective spectrograms (f,g,h).

dard, 2015]. Therefore the ray-paths and eigenrays presented here are likely an oversimplified representation of the true paths taken by the acoustic waves before their detection at the ULDB. Future studies of acoustic wavefields generated by lightning infrasound must take into account the complex refraction patterns induced by vertical columns of wind shear within thunderclouds.

The measured waveforms do not display the compression-rarefaction-compression shape that had been modeled as generated by a rapid intensification and discharge of the electric field in the thundercloud [*Pasko*, 2009]. It must be noted that the waveforms modeled by *Pasko* [2009] are of 0.1-1 Hz frequency and the acoustic wavefield was strongly oriented in the vertical direction [*Dessler*, 1973]. The detection of lightning infrasound from strokes at more than several tens of kilometers from the ULDB does not support the theory that acoustic wavefields generated by lightning infrasound are strictly orientated vertically. Instead, the waveforms here share amplitude, frequency and range detection characteristics with previously recorded lightning infrasound signals which were attributed to charge deposition in the lightning channels [e.g. *Farges and Blanc*, 2010; *Arechiga et al.*, 2014].

The observations here of lightning infrasound recorded by a high-altitude balloon over the Tasman Sea in May 2016 are fortuitous. Yet, they also demonstrate the potential for using these platforms to fill gaps on our monitoring capabilities of infrasound generating sources such as lightning storms. Future high-altitude balloon deployments combined with ground-based instruments will be required to image the full infrasonic wavefield generated by thunderstorms which, in turn, will provide a better understanding of the source mechanics of lightning infrasound. Furthermore, acoustic source localization is possible by the simultaneous deployment of multiple balloons to form a high-altitude, free-flying acoustic network [e.g. *Bowman and Albert*, 2018].

Acknowledgments

We would like to thank the NASA Balloon Program Office and the NASA Columbia Scientific Ballooning Facility for hosting our instrumentation on the 2016 Ultra Long Duration Balloon Mission. The authors also wish to thank the World Wide Lightning Location Network (http://wwlln.net), a collaboration including over 50 institutions, for providing the lightning data used in this paper. The acoustic data presented here is accessible at datadryad.org under the following doi: 10.5061/dryad.40877s4. This work was supported by National Science Foundation Grant AGS-1551999. Sandia National Laboratories is a multi-mission laboratory managed and operated by National Technology and Engineering Solutions of Sandia, LLC., a wholly owned subsidiary of Honeywell International, Inc., for the U.S. Department of Energy's National Nuclear Security Administration under contract DE-NA0003525. The views expressed here do not necessarily reflect the views of the United States Government, the United States Department of Energy, or Sandia National Laboratories.

References

Anderson, J. F., J. B. Johnson, R. O. Arechiga, and R. J. Thomas (2014), Mapping thunder sources by inverting acoustic and electromagnetic observations, *Journal of Geophysical Research: Atmospheres*, *119*(23), 13,287–13,304, doi: 10.1002/2014JD021624.

Anderson, W. J., and I. Taback (1991), Oscillation of High-Altitude Balloons, *Journal of Aircraft*, *28*(9), 606–608.

Arechiga, R., M. Stock, R. Thomas, H. Erives, W. Rison, H. Edens, and J. Lapierre (2014), Location and analysis of acoustic infrasound pulses in lightning, *Geophysical Research Letters*, *41*(13), 4735–4744, doi:10.1002/2014GL060375.

Assink, J. D., L. G. Evers, I. Holleman, and H. Paulssen (2008), Characterization of infrasound from lightning, *Geophysical Research Letters*, *35*(15), 1–5, doi: 10.1029/2008GL034193.

Balachandran, N. K. (1983), Acoustic and electric signals from lightning, *Journal of Geophysical Research: Oceans*, *88*(C6), 3879–3884, doi:10.1029/JC088iC06p03879.

Behnke, S. A., and S. R. McNutt (2014), Using lightning observations as a volcanic eruption monitoring tool, *Bulletin of Volcanology*, *76*(847), doi:10.1007/s00445-014-0847-1.

Blackstock, D. (2000), *Fundamentals of Physical Acoustics*, John Wiley and Sons.

Blanc, E., A. Le Pichon, L. Ceranna, T. Farges, J. Marty, and P. Herry (2010), Global Scale Monitoring of Acoustic and Gravity Waves for the Study of the Atmospheric Dynamics, in *Infrasound Monitoring for Atmospheric Studies*, edited by

A. Le Pichon, E. Blanc, and A. Hauchecorne, pp. 647–664, Springer Netherlands, Dordrecht.

Blom, P., and R. Waxler (2012), Impulse propagation in the nocturnal boundary layer: Analysis of the geometric component, *The Journal of the Acoustical Society of America*, *131*(5), 3680–3690, doi:10.1121/1.3699174.

Bohannon, J. L., A. A. Few, and A. J. Dessler (1977), Detection of Infrasonic Pulses from Thunderclouds, *Geophysical Research Letters*, *4*(2), 49–52.

Bowman, D. C., and S. A. Albert (2018), Acoustic Event Location and Background Noise Characterization on a Free Flying Infrasound Sensor Network in the Stratosphere, *Geophysical Journal International*, doi:10.1093/gji/ggy069.

Bowman, D. C., and J. M. Lees (2015), Infrasound in the middle stratosphere measured with a free-flying acoustic array, *Geophysical Research Letters*, *42*(22), 10,010–10,017, doi:10.1002/2015GL066570.

Bowman, D. C., and J. M. Lees (2017), A Comparison of the Ocean Microbarom Recorded on the Ground and in the Stratosphere, *Journal of Geophysical Research: Atmospheres*, *122*(18), 9773–9782, doi:10.1002/2017JD026474.

Bowman, D. C., and J. M. Lees (2018), Upper atmosphere heating from ocean-generated acoustic wave energy, *Geophysical Research Letters*.

Bowman, D. C., J. M. Lees, J. A. Cutts, E. F. Young, K. T. Seiffert, M. Boslough, and S. J. Arrowsmith (2017), Geoacoustic Observations on Drifting Balloon-Borne Sensors, in *Infrasound Monitoring for Atmospheric Studies*, edited by A. Le Pichon, E. Blanc, and A. Hauchecorne, 2 ed.

Campus, P., and D. Christie (2010), Worldwide Observations of Infrasonic Waves, in *Infrasound Monitoring for Atmospheric Studies*, edited by A. Le Pichon, E. Blanc, and A. Hauchecorne, pp. 185–234, Springer Netherlands.

Christie, D. R., and P. Campus (2010), The IMS Infrasound Network: Design and Establishment of Infrasound Stations, in *Infrasound Monitoring for Atmospheric Studies*, edited by A. Le Pichon, E. Blanc, and A. Hauchecorne, pp. 29–75, Springer Netherlands.

Dessler, A. J. (1973), Infrasonic thunder, *J. Geophys. Res.*, *78*(12), 1889–1896, doi:10.1029/JC078i012p01889.

Dowden, R. L., R. H. Holzworth, C. J. Rodger, J. Lichtenberger, N. R. Thomson, A. R. Jacobson, E. Lay, J. B. Brundell, T. J. Lyons, S. O'Keefe, Z. Kawasaki, C. Price, V. Prior, P. Ortéga, J. Weinman, Y. Mikhailov, O. Veliz, X. Qie, G. Burns, A. Collier, O. Pinto Junior, R. Diaz, C. Adamo, E. R. Williams, S. Kumar, G. B. Raga, J. M. Rosado, E. E. Avila, M. E. Clilvera, T. Ulich, P. Gorham, T. J. G. Shanahan, T. Osipowicz, G. Cook, and Y. Zhao (2008), World-Wide Lightning Location Using VLF Propagation in the Earth-Ionosphere Waveguide, *IEEE Antennas and Propagation Magazine*, *50*(5), 40–60.

Farges, T., and E. Blanc (2010), Characteristics of infrasound from lightning and sprites near thunderstorm areas, *Journal of Geophysical Research: Space Physics*, *115*(A6), doi:10.1029/2009JA014700.

Fee, D., and R. S. Matoza (2013), An overview of volcano infrasound: From hawaiian to plinian, local to global, *Journal of Volcanology and Geothermal Research*, *249*, 123–139, doi:10.1016/j.jvolgeores.2012.09.002.

Few, A., A. Dessler, D. Latham, and M. Brook (1967), A dominant 200-hertz peak in the acoustic spectrum of thunder, *Journal of Geophysical Research*, *72*(24), 6149–6154.

Hutchins, M. L., R. H. Holzworth, C. J. Rodger, and J. B. Brundell (2012), Far-Field power of lightning strokes as measured by the world wide lightning location network, *Journal of Atmospheric and Oceanic Technology*, *29*(8), 1102–1110, doi:10.1175/JTECH-D-11-00174.1.

Jones, R. M., and A. J. Bedard (2015), Infrasonic ray tracing applied to small-scale atmospheric structures: Thermal plumes and updrafts/downdrafts, *The Journal of* *the Acoustical Society of America*, *137*(2), 625–632, doi:10.1121/1.4906175.

Kim, K., and J. M. Lees (2014), Local Volcano Infrasound and Source Localization Investigated by 3D Simulation, *Seismological Research Letters*, *85*(6), 1177–1186, doi:10.1785/0220140029.

Lacanna, G., and M. Ripepe (2013), Influence of near-source volcano topography on the acoustic wavefield and implication for source modeling, *Journal of Volcanology and Geothermal Research*, *250*, 9–18, doi:10.1016/j.jvolgeores.2012.10.005.

Marcillo, O., J. B. Johnson, and D. Hart (2012), Implementation, characterization, and evaluation of an inexpensive low-power low-noise infrasound sensor based on a micromachined differential pressure transducer and a mechanical filter, *Journal of Atmospheric and Oceanic Technology*, *29*(9), 1275–1284, doi:10.1175/JTECH-D-11-00101.1.

Pasko, V. P. (2009), Mechanism of lightning-associated infrasonic pulses from thunderclouds, *Journal of Geophysical Research Atmospheres*, *114*(8), 1–10, doi:10.1029/2008JD011145.